Hindawi Publishing Corporation
Journal of Control Science and Engineering
Volume 2011, Article ID 783741, 12 pages
doi:10.1155/2011/783741

Research Article

An Approach to Stable Walking over Uneven Terrain Using a Reflex-Based Adaptive Gait

Umar Asif[1, 2] and Javaid Iqbal[1, 2]

[1] *National University of Sciences and Technology, Islamabad 44000, Pakistan*
[2] *Mechatronics Engineering Department, College of Electrical & Mechanical Engineering, Peshawar Road, Rawalpindi 46000, Pakistan*

Correspondence should be addressed to Umar Asif, umar.asif@unswalumni.com

Received 9 February 2011; Revised 25 April 2011; Accepted 25 May 2011

Academic Editor: Zhiyong Chen

This paper describes the implementation of an adaptive gait in a six-legged walking robot that is capable of generating reactive stepping actions with the same underlying control methodology as an insect for stable walking over uneven terrains. The proposed method of gait generation uses feedback data from onboard sensors to generate an adaptive gait in order to surmount obstacles, gaps and perform stable walking. The paper addresses its implementation through simulations in a visual dynamic simulation environment. Finally the paper draws conclusions about the significance and performance of the proposed gait in terms of tracking errors while navigating in difficult terrains.

1. Introduction

In the field of motion planning for legged robots, a large body of research work is inspired from insects due to the fact that they are responsive, adaptive and possess sensory systems to generate reactive walking patterns [1]. In the field of biomimetic robots, a large volume of work [2–6] exists which deals with their modeling and design inspired from legged creatures found in nature.

It has been well understood through various research studies that mammals and walking insects posses inherent capabilities to choose stable and secure walking patterns in response to external disturbances when the terrain becomes uneven to keep up a continuous gait. This walking pattern is characterized by the sequential motion of legs and coordinated advancement of the body which makes them appropriate and suitable for replicating in walking robots for the real world. A wave gait is the typical gait which is considered to possess intrinsic terrain adaptability. On the other hand, a tripod gait [7] is well known for walking with high mobility due to its fast gait speed and greater static stability.

1.1. Literature Review and Related Work. In the field of navigation in difficult terrains, a large volume of research work deals with the development of terrain adaptation control algorithms to realize efficient and stable locomotion [8–10]. Among few works, a motion planner based on a distributed neural network controller [11], gait generation methods using energy-based stability margins to understand reliable locomotion [12], fault detection schemes [13], development of fault tolerant cyclic gaits [14], and gait planning based upon kinematic control of hexapod robots [15] are some investigations with excellent results.

Earlier robot designs such as [16] focused on the development of behavior based strategies to formulate the robot-environment interactions in order to design adaptive walking behaviors using sensory information. Later on, studies such as [17–19] investigated the design of robotic systems with their prime objective to realize the walking behaviors of insects in real walking machines. Thus, the objective of these research studies has always been an effort to devise schemes to define leg movements which replicate those of actual insects in order to realize biologically inspired walking. Curse worked on such gait generation methodologies by investigating the walking behaviors of stick insects [20, 21]. An appreciable contribution in this context was made by the researchers Hess and Büschges [22] and Ekeberg et al. [1], who studied the insect neurobiology and investigated that the stick insects control their leg movements through sensory oscillators in their joints and thoracic ganglia. Therefore,

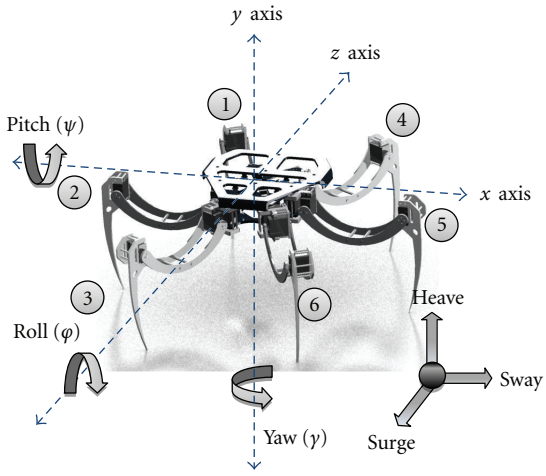

Figure 1: Pro engineer model of hexapod robot.

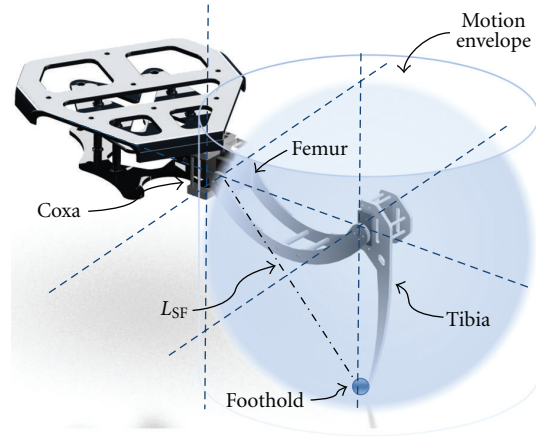

Figure 2: Structure of an individual leg.

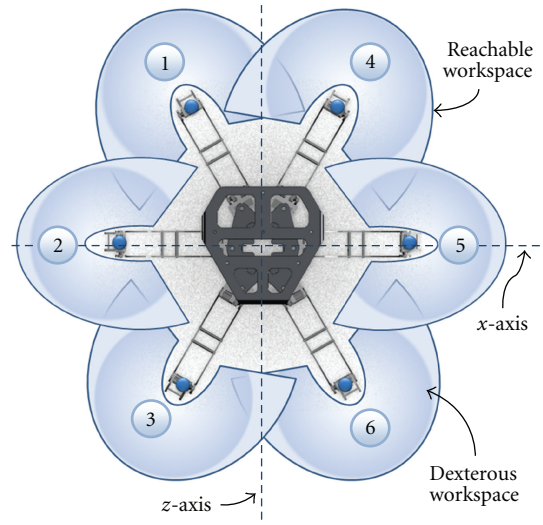

Figure 3: Working envelopes of robot legs.

their joint movements in a particular leg are influenced by sensory signals from the brain as well as from the joints in other legs to generate reactive stepping patterns. Since, the patterns are reactive the resulting locomotion is responsive and adaptive that allows the insect to conform to its underlying terrain. Such neurobiological-based gait generation methodologies have been realized using computer simulations [1] with one and two legged robots [23]. A closely related study [24] deals with an excellent implementation of such a neurobiological leg control system identified in the thoracic ganglia of stick insects using a hexapod robot by modeling biologically plausible sensory pathways for pattern generation. The work [24] describes these pathways using advanced algorithm like "Elevator Reflex" to surmount obstacles and "Searching Reflex" to surmount gaps and holes in order to improve navigation over rough terrains with excellent results.

While these research investigations are sufficient to demonstrate the success of adaptive locomotion, most of the work deals with implementation on either smooth flat surfaces or structured environments only. In natural terrains, the formation of impulsive forces during the impact (robot-ground interaction) giving rise to disturbances, affects the walking gait and offers a great challenge to realize locomotion with adequate stability and performance. Therefore, in contrast, this paper aims to describe a biologically inspired gait generation method for walking over uneven terrains with an ability to traverse through obstacles and gaps with minimal tracking errors.

The first part of the paper describes our six-legged robot in terms of its modeling and design. The second part of the paper describes our proposed foothold reflex control method to generate a reactive and adaptive gait, able to plan footholds and appropriate leg sequences to change support points and transverse a rough terrain.

2. Robot Modeling and Design

2.1. Physical Model. The mechanical structure of our robot as shown in Figure 1, consists of six identical legs placed around the main body in a biologically inspired configuration to enable omni-directionability and enhance maneuverability. In order to describe the kinematic model of the robot leg inspired from a stick insect, the work presented in [25] has been reviewed. There are four functional segments of the leg of a stick insect: the coxa (c), the femur (f), the tibia (t), and the foot. For simplicity, a stick insect leg can be modelled as a serial manipulator with three hinge joints by neglecting the joint of the foot and the foot itself, resulting in three degrees of freedom as investigated in [25]. Thus, the leg of our robot consists of three links namely: coxa, femur and tibia, interconnected through three revolute joints. From the body towards the foot, the joints are called body-coxa joint (θ_c), coxa-femur joint (θ_f), and femur-tibia joint (θ_t). Figure 2 portraits the kinematic configuration of the leg in terms of its links and their motion envelope.

2.2. Reachable Workspace. If all the joints of a leg return appropriate or desirable angles for a reference pose in a given space, then that pose is considered to be a subset of

manipulator's working space. In this context, analytic and diagrammatizing methods are typically used to work out the robot's working space. On the other hand, the numerical methods have advantages such as fast speed, high precision, easy operation, large application range, and adaptability to various types of robotic structures. As a consequence, it is widely used by researchers as investigated in [26, 28].

Figure 3 shows the working envelopes of all the legs attached to the main body as a reachable workspace represented by solid annulus regions. Each leg has a reachable area in the form of a sector as defined in [29], where adjacent or neighboring areas cause overlap of each other's region. Thus, for avoiding the interference problem, a dexterous workspace is determined contained inside the reachable workspace of each leg as shown in the Figures 2 and 3. The dexterous workspace is an area on the plane mapped on the terrain within which a leg can be placed effectively anywhere while satisfying the static stability.

2.3. Kinematic Model. The kinematic model of our robot consists of forward and inverse kinematic equations formulated using Denavit-Hartenberg convention as investigated in [30], further described by (1).

$$
\begin{aligned}
\mathrm{Foot}_{x_i}^{G} &= \cos\gamma\cos\varphi {Px_{ft_i}}^{B} - \cos\gamma\sin\varphi {Py_{ft_i}}^{B} + \sin\gamma {Pz_{ft_i}}^{B},\\
\mathrm{Foot}_{y_i}^{G} &= (\cos\psi\sin\varphi + \sin\psi\sin\gamma\cos\varphi){Px_{ft_i}}^{B} + (\cos\psi\cos\varphi - \sin\psi\sin\gamma\sin\varphi){Py_{ft_i}}^{B}\\
&\quad - \sin\psi\cos\gamma {Pz_{ft_i}}^{B},\\
\mathrm{Foot}_{z_i}^{G} &= (\sin\psi\sin\varphi - \cos\psi\sin\gamma\cos\varphi){Px_{ft_i}}^{B} + (\sin\psi\cos\varphi + \cos\psi\sin\gamma\sin\varphi){Py_{ft_i}}^{B}\\
&\quad + \cos\psi\cos\gamma {Pz_{ft_i}}^{B},\\
\theta_{ci} &= \mathrm{ATAN2}\left(\mathrm{Foot}_{z_i}^{G}, \mathrm{Foot}_{x_i}^{G}\right),\\
\theta_{fi} &= \mathrm{ATAN2}\left(t_i, -\mathrm{Foot}_{y_i}^{G}\right)\\
&\quad + \mathrm{ATAN2}\left(\left(\sqrt{-{\mathrm{Foot}_{y_i}^{G}}^2 + {t_i}^2 - \frac{\left({t_i}^2 + {l_f}^2 + {\mathrm{Foot}_{y_i}^{G}}^2 - {l_t}^2\right)^2}{2\times l_f}}\right),\right.\\
&\qquad \left.\frac{\left({t_i}^2 + {l_f}^2 + {\mathrm{Foot}_{y_i}^{G}}^2 - {l_t}^2\right)}{2\times l_f}\right),\\
\theta_{ti} &= \mathrm{ATAN2}\left(\left(-\mathrm{Foot}_{y_i}^{G}\cos\theta_f - \sin\theta_f t_i\right), \left(t_i\cos\theta_f - l_f - \sin\theta_f \mathrm{Foot}_{y_i}^{G}\right)\right),\\
t_i &= \mathrm{Foot}_{x_i}^{G}\cos\theta_c - l_c + \mathrm{Foot}_{z_i}^{G}\sin\theta_c,\\
\mathrm{CoM}_i^{G} &= \frac{\sum m_i \times p_{\mathrm{CoM}_i^{G}}}{\sum m_i},\\
x_{i\mathrm{ZMP}} &= \frac{\sum_{i=1}^{n} m_i\left(x_i\left(\ddot{y}_i + g_y\right) - \ddot{x}_i y_i\right)}{\sum_{i=1}^{n} m_i x_i\left(\ddot{y}_i + g_y\right)},\\
z_{i\mathrm{ZMP}} &= \frac{\sum_{i=1}^{n} m_i\left(z_i\left(\ddot{y}_i + g_y\right) - \ddot{z}_i y_i\right)}{\sum_{i=1}^{n} m_i z_i\left(\ddot{y}_i + g_y\right)},\\
m_i &= \text{mass of the link } i;\\
x_i, y_i, z_i &= \text{position vector of link } i;\\
\ddot{x}_i, \ddot{y}_i, \ddot{z}_i &= \text{accelerations of link } i;\\
g_y &= \text{gravity vector;}\\
\mathrm{CoM}_i^{G} &= \text{center of mass of link } i;\\
[x_{i\mathrm{ZMP}}\ z_{i\mathrm{ZMP}}] &= \text{zero moment point position vector;}\\
\left[\mathrm{Foot}_{x_i}^{G}\ \mathrm{Foot}_{y_i}^{G}\ \mathrm{Foot}_{z_i}^{G}\right] &= \text{foothold position vector;}\\
\left[\theta_{ci},\ \theta_{fi},\ \theta_{ti}\right] &= \overline{q}_i = \text{joints rotation angles.}
\end{aligned}
\tag{1}
$$

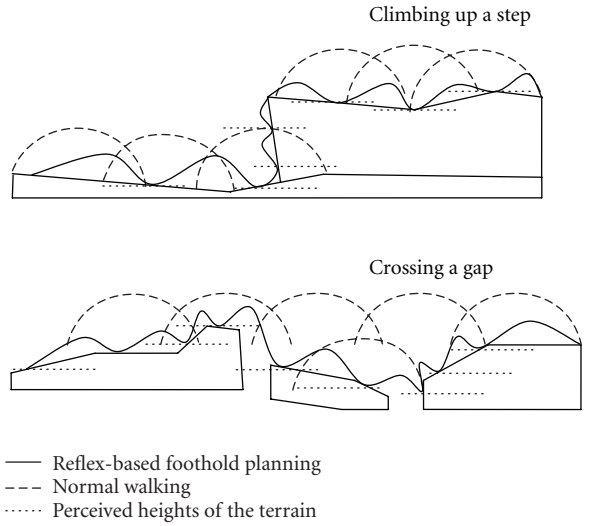

Figure 4: Climbing a step (top) and crossing gaps (bottom) scenarios to present the foothold planning using the proposed Foothold Reflex Control method. Normal walking behavior is momentarily changed upon sensing an obstruction. Once the obstruction is removed (e.g., loss of contact with the obstruction), the normal motions are resumed.

In order to ensure the performance of a walking gait, the performance measures are typically evaluated in terms of gait stability margins using zero moment point (ZMP) based stability criterion. Therefore, it is necessary to consider and define the ZMP-based stability criterion. The definition of ZMP adopted in this paper is as described in [31, 32], which is: ZMP is the projected point of the resultant forces of the gravity and the inertia forces acting on the robot to the ground, to which the moments of the resultant forces equal to zero. To ensure dynamic stability, the ZMP must lie within the Support Polygon on Surface (SPOS) at all the times and does not lie on the edges of the SPOS. SPOS is the convex hull (polygon) of the footholds in contact with the ground. If the ZMP reaches the edge of the SPOS, the walking gait will develop a high tendency to become unstable and may result in tumbling of the robot on the ground. The position of ZMP is derived from [31, 32], as described in (1).

3. Terrain Adaptation

Terrain exploration is considered to be an important aspect in motion planning of walking robots that has been previously discussed in more detail in [33–40]. Once a terrain map is available, a foothold selection method can be implemented. In this paper, the terrain knowledge is supplied to the robot offline in form of terrain's latitude, longitude, and altitude information. The objective is to follow a reference path on a known geographical location using its latitude, longitude, and altitude information. During walking, the robot uses sensor-based traction control to perform straight line walking.

3.1. Gait Generation. The gait modeled here constitutes three phases: swing, drop, and stance as described in (2). Each phase is characterized by its unique combination of leg and joint motions coordination. Swing is identified by protraction of body-coxa joint, levation of the coxa-femur joint, and extension of the femur-tibia joint. This combination serves to lift the foothold from $\text{Foot}_{y_i}^{G}$ to $\text{Foot}_{y_{i+1}}^{G}$ and sway it in the direction of motion to acquire the next foothold position $(\text{Foot}_{x_{i+1}}^{G}, \text{Foot}_{z_{i+1}}^{G})$ in air. Drop phase lowers the leg until contact with ground is verified from foothold's touch sensor notification. During stance phase, the involved legs both support and propel the body in the direction of desired motion. Joint trajectories $(\overline{q}_i, \dot{\overline{q}}_i, \ddot{\overline{q}}_i)$ are computed using linear splines with parabolic blends as described in (2).

$$
\begin{aligned}
\text{Swing} &= f\left(\overline{q}_i\right)(\text{leglift}, \text{legstroke}),\\
&0 < \text{leglift} \le 15\,\text{cm},\\
&0 < \text{legstroke} \le 10\,\text{cm},\\
\text{Stance} &= f\left(\overline{q}_i\right)(\text{duty factor } (\beta), \text{legstroke}),\\
\text{leglift} &= \text{Foot}_{y_i}^{G} \overset{\Delta}{\rightarrow} \text{Foot}_{y_{i+1}}^{G},\\
\text{legstroke} &= \begin{cases} \text{Foot}_{x_i}^{G} \overset{\Delta}{\rightarrow} \text{Foot}_{x_{i+1}}^{G}, \\ \text{Foot}_{z_i}^{G} \overset{\Delta}{\rightarrow} \text{Foot}_{z_{i+1}}^{G}, \end{cases}\\
\text{Gait Speed} &= S_i = \frac{\delta_{i+1} - \delta_i}{t_{i+1} - t_i},\\
\beta &= \frac{t_{\text{stance}}}{t_{\text{cycle}}}, \quad \left(\beta\omega_{\text{swing}} + \beta\omega_{\text{stance}} = 1\right),\\
\text{linear spline} &\begin{cases} \overline{q}_i = \overline{q}_{i+1} + \left(\dot{\overline{q}}_{i+2} - \dot{\overline{q}}_{i+1}\right)t_i, \\ \dot{\overline{q}}_i = \dot{\overline{q}}_{i+2} - \dot{\overline{q}}_{i+1}, \\ \ddot{\overline{q}}_i = 0, \end{cases}\\
\text{parabolic blend} &\begin{cases} \overline{q}_i = \overline{q}_{i+1} \\ \qquad + \left(\dot{\overline{q}}_{i+2} - \dot{\overline{q}}_{i+1}\right)(t_i - t_{\text{blend}}) \\ \qquad + \frac{1}{2}\ddot{\overline{q}}_{i+2}{t_{\text{blend}}}^2 \\ \dot{\overline{q}}_i = \dot{\overline{q}}_{i+2} - \dot{\overline{q}}_{i+1} + \ddot{\overline{q}}_{i+2}t_{\text{blend}} \\ \ddot{\overline{q}}_i = \ddot{\overline{q}}_{i+2} \\ t_{\text{blend}} = t_i - \left(\frac{1}{2}t_{i+1} + (t_{i+2} - t_{i+1})\right) \end{cases}\\
\omega_{\text{swing}} &= \text{swing frequency};\\
\omega_{\text{stance}} &= \text{stance frequency};\\
t_{\text{cycle}} &= \text{total cycle time};\\
t_{\text{stance}} &= \text{stance time};\\
\delta_i &= \text{distance travelled}.
\end{aligned}
\tag{2}
$$

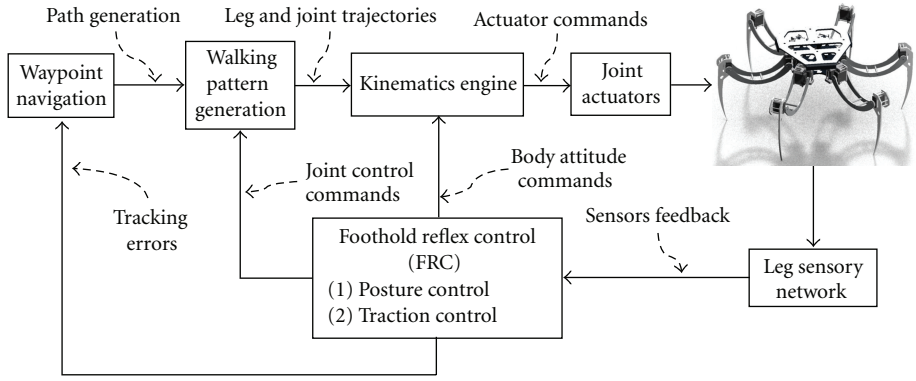

Figure 5: Overall control system framework.

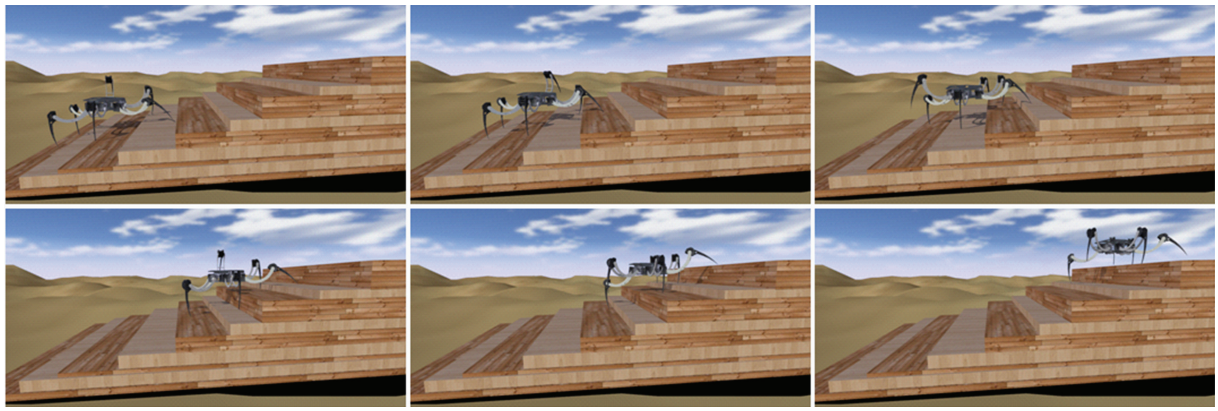

Figure 6: Pictorial representation of robot climbing steps of variable heights using Foothold Reflex Control (FRC) method.

As described earlier, a leg sensory network is established for each leg that defines a reflex system to inform the main controller that a disturbance requiring a behavior other than normal walking has been encountered. Upon perceiving such an abnormal behavior, the controller generates sensory information based upon disturbance estimation during the impact (leg-environment interaction) that alters the normal sequential motion of joints to adaptive and emergent. This reflex-based gait generation method is termed as foothold reflex control (FRC), further explained in the following Section 3.2.

3.2. Foothold Reflex Control (FRC). The Foothold Reflex Control (FRC) method aims to step over surmountable obstacles, sizeable gaps and holes using online traction control. The method makes an estimate of the terrain by using the foot contact point information from the leg sensory network. If all the contact points are at the same height, the robot is considered to be walking on a flat terrain. In such a case, the robot uses a short *leglift* and a large *legstroke* to increase its travel speed.

Upon detecting a step or a surmountable obstacle using the sensor information, the FRC initiates the behavior other than normal walking that alters the motions of the involved leg to retraction to a safe zone (an attempt to minimize the risk of snagging on the obstacle), levation in air (an effort to acquire a position higher than the perceived height of the obstacle), and swing to its next foothold planned within the dexterous workspace of the involved leg. In parallel, FRC uses an independent attitude controller to keep the robot's body leveled above the terrain with online adjustments while climbing and traversing over the gaps using a sensor-based traction control. This phenomenon is further illustrated in Figure 4 using dynamic simulation results in order to validate the success of the proposed method.

Foot interaction with the ground is modeled here based on a general coulomb friction model [41, 42], further described in (3).

$$\begin{bmatrix} \text{Foot}_{x_{i+1}}^{G} \\ \text{Foot}_{z_{i+1}}^{G} \end{bmatrix} = \begin{bmatrix} \text{Foot}_{x_i}^{G} \\ \text{Foot}_{z_i}^{G} \end{bmatrix} + \begin{bmatrix} \iint_i^{i+1} \dfrac{f_{x_i} + m_i \ddot{x}_i}{m_i} \\ \iint_i^{i+1} \dfrac{f_{z_i} + m_i \ddot{z}_i}{m_i} \end{bmatrix},$$

$$F_{ti} \leq \mu N_i, \tag{3}$$

$$\sqrt{f_{x_i}^2 + f_{z_i}^2} - \mu N_i < 0,$$

where F_{ti} is the total tangential force between the contact point and the terrain, μ is the combined coefficient of ground

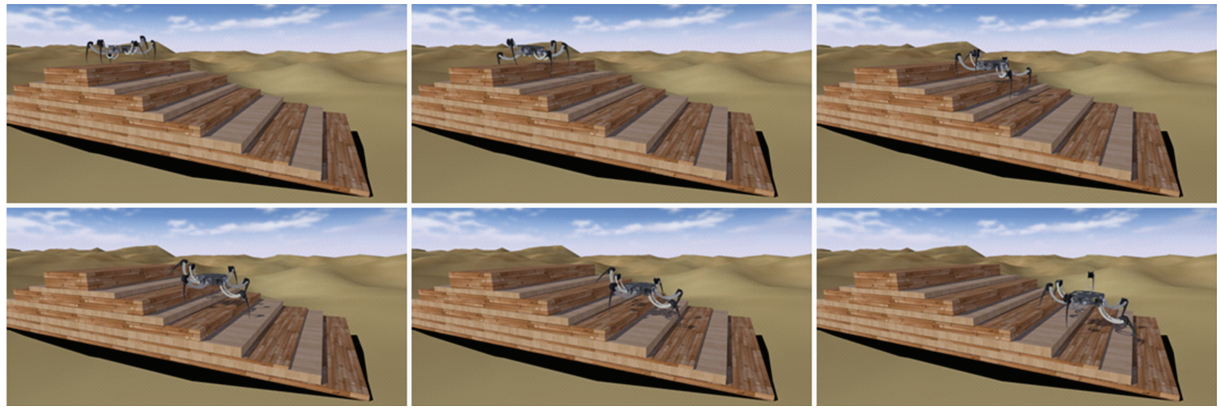

Figure 7: Pictorial representation of robot descending steps of variable depths using Foothold Reflex Control (FRC) method.

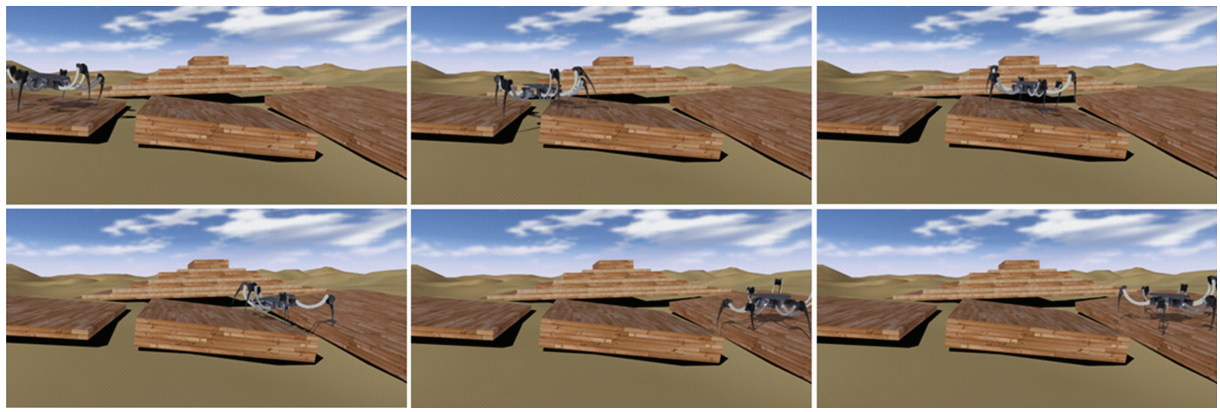

Figure 8: Pictorial representation of robot traversing through gaps of variable gap lengths using Foothold Reflex Control (FRC) method.

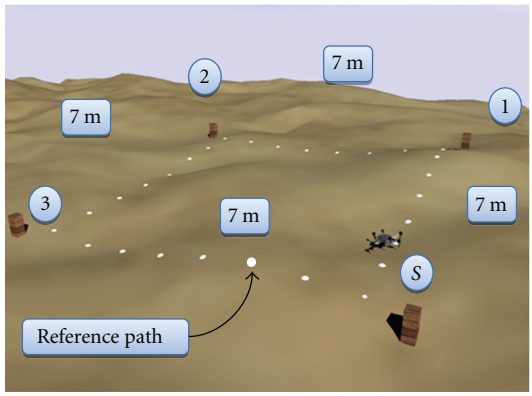

Figure 9: Terrain created using heightfield maps in a dynamic simulation environment.

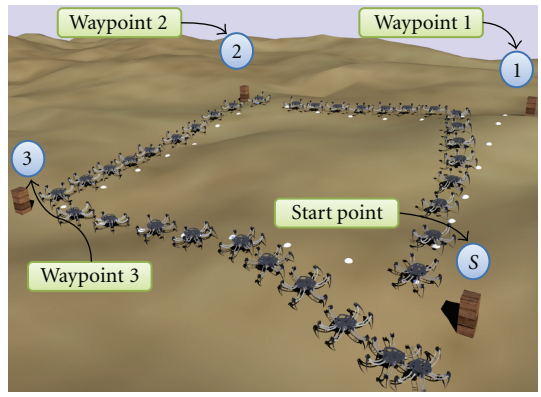

Figure 10: Pictorial representation of the path traced by the robot without using the FRC method.

static and dynamic friction, and N_i is the total normal reaction force to prevent the penetration of the contact point. The coefficients of static and dynamic friction are taken as a combined coefficient of ground friction for simplicity, calculated online using the tangential and normal reaction forces estimated using leg sensors data. The overall control framework is further illustrated in Figure 5.

3.3. Gait Performance Measures. To be able to generate an optimal gait, it is necessary to determine the performance of the proposed gait generation. In this paper, the performance of the gait is chosen to be measured on the traction of the robot and its stability. As described earlier, the stability of the robot is determined online by evaluating the position of the CoM and ZMP relative to the SPOS.

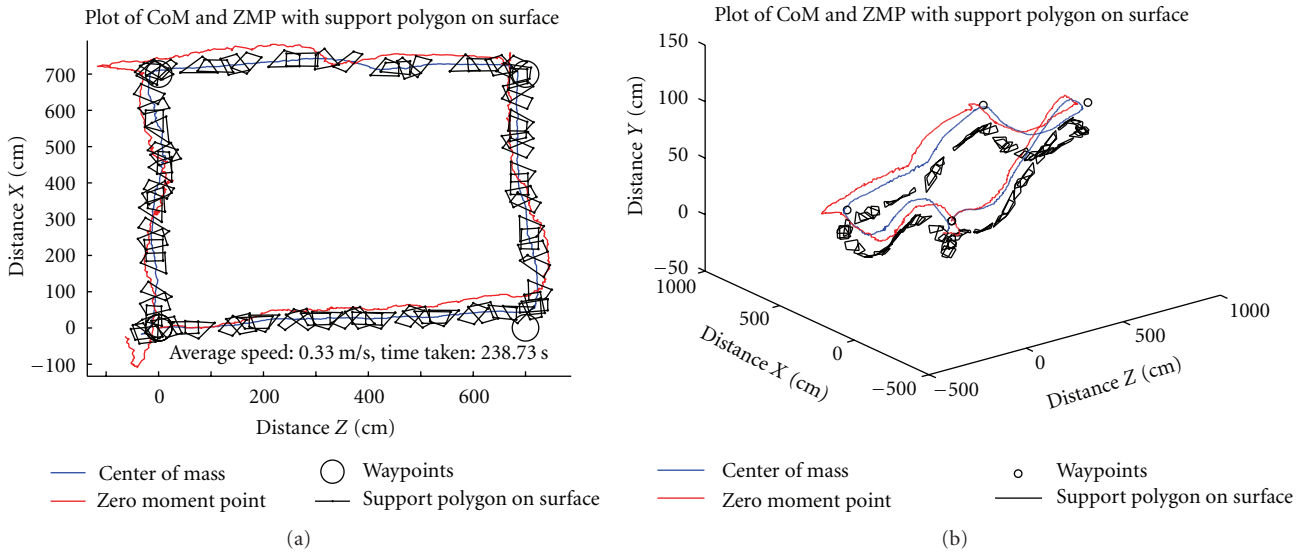

Figure 11: Plot of CoM and ZMP with SPOS without using the Foothold Reflex Control method.

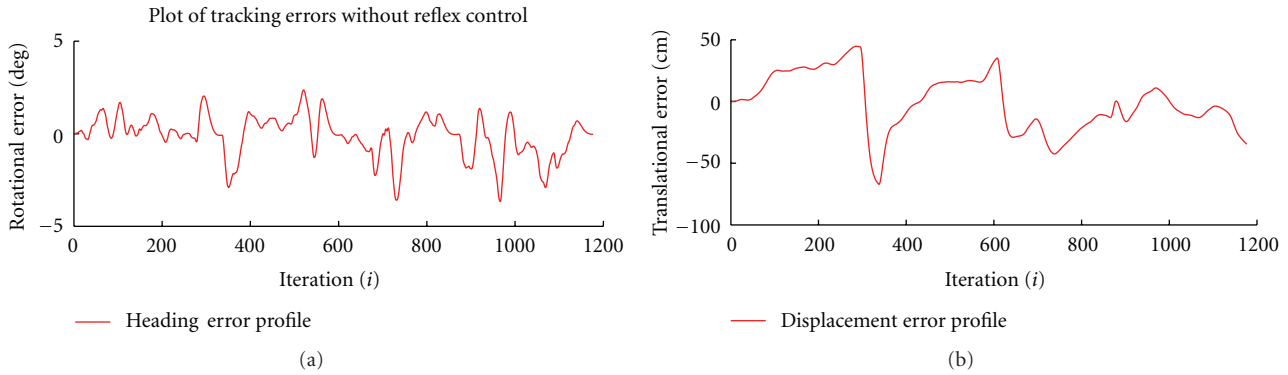

Figure 12: Tracking errors of robot locomotion without using the FRC method.

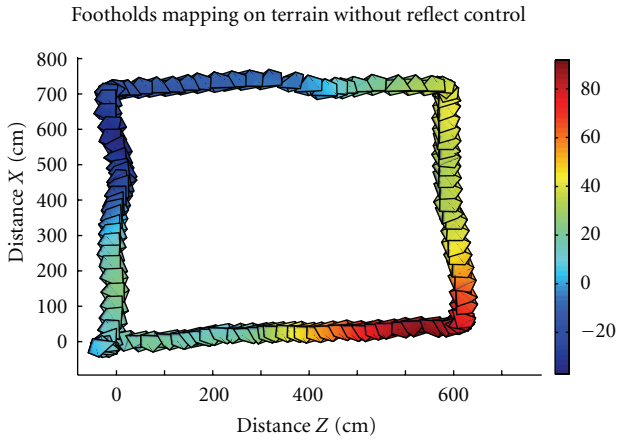

Figure 13: Terrain intercepted by the robot without using the FRC method.

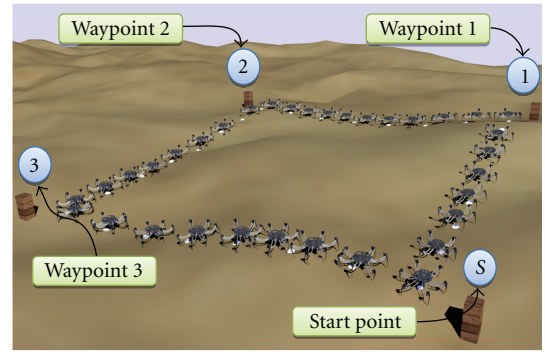

Figure 14: Pictorial representation of the path traced by the robot using the proposed FRC method.

4. Simulation Results

Initial simulation tests were performed to realize the success of the FRC method to traverse through steps and gaps as illustrated in Figure 4. Pictorial representation of the robot climbing and descending steps is further shown in Figures 6 and 7 while traversing over gaps is pictorially illustrated in Figure 8.

4.1. Obstacle Crossing Testing. During these tests, the robot was able to walk with a maximum speed of 5 cm/sec.

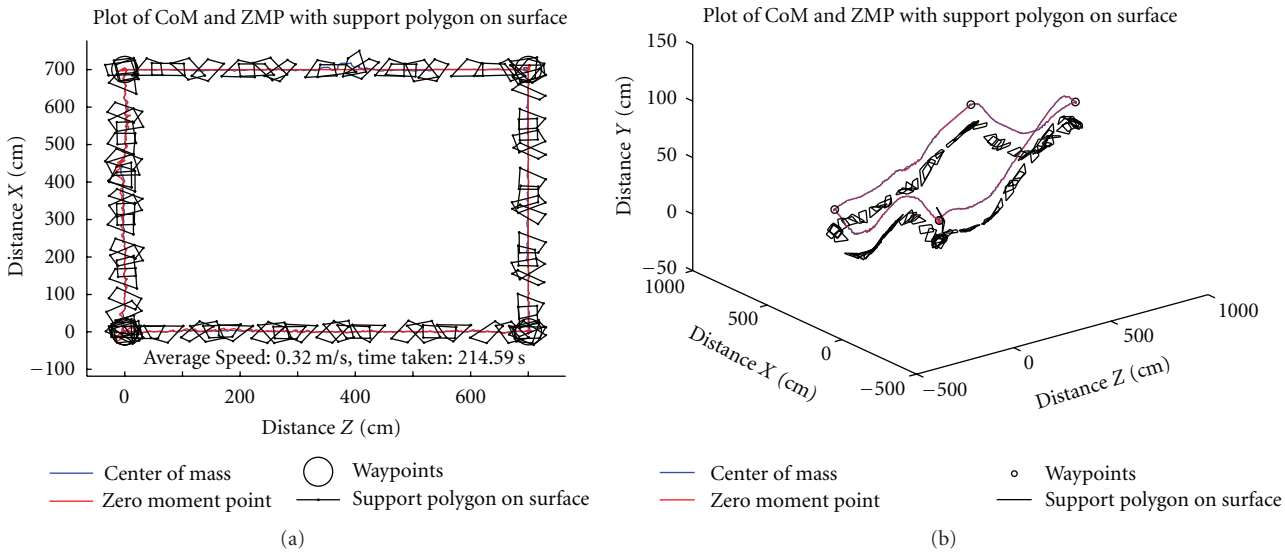

Figure 15: Plot of CoM and ZMP with SPOS using the proposed Foothold Reflex Control method.

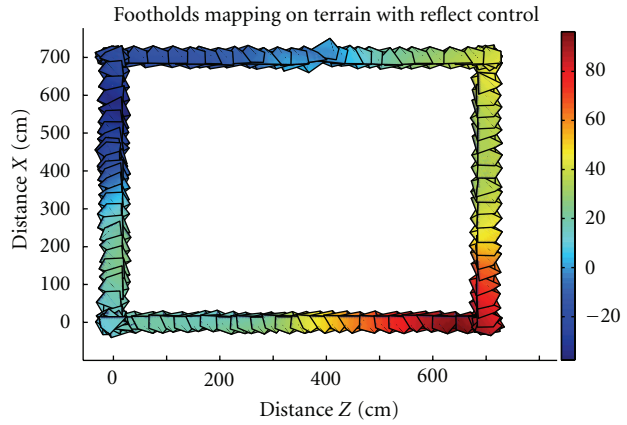

Figure 16: Terrain intercepted by the robot using the FRC method.

The robot started with control inputs (leg-lift: 9 cm and leg-stroke: 5 cm) and easily surmounted the initial steps (step heights: 3 cm, 5 cm, 2 cm, 6 cm, 7 cm) without much modification to the planned control variables. Upon perceiving obstruction (step height: 10 cm), the leg retracted 2 cm, levated 6 cm, and extended with a leg-stroke of 7 cm as a consequence of the Foothold Reflex Control method intervention. As this leg-lift of 6 cm was still insufficient to clear the obstacle, the contact switch again detected the surface and the FRC sequential loop re-executed. The robot surpassed the obstruction eventually with a leg-lift of 12 cm and leg-stroke of 7 cm. Similarly, upon detecting obstruction (step height: 15 cm), the leg was elevated 20 cm which was the maximum achievable leg-lift within its dexterous workspace to surmount obstacle. The robot successfully steered through the rest of the descending steps using the same methodology. Raised surfaces of variable widths and variable heights were placed over an uneven terrain perpendicular to the robot's path of motion in order to test the ability of the controller in navigating through gaps and holes. The first gap was approximately 5 cm deep and 7 cm across, while the second gap was 7 cm deep and 9 cm across. Success was observed in most of the simulation trials.

4.2. Walking over Uneven Terrain Testing. In order to evaluate the performance of the proposed FRC method for navigation in irregular terrains, a terrain is setup using dynamic simulation environment provided by Microsoft Robotics Developer Studio. The terrain constitutes an uneven surface-mesh created using heightfield maps to model elevations and depressions which can offer significant disturbances while walking, as shown in Figure 9. This terrain offers a big challenge in comparison to flat surfaces in terms of stable locomotion because the elevations and depressions subject the robot to a large deal of disturbances in both lateral and angular directions.

In the first simulation test, the FRC method was not used. Figure 11 shows the locomotion of the robot in terms of its center of mass (CoM) and zero moment point (ZMP) profiles with the support polygons on surface. As apparent from the figures, when the FRC method was not used, the robot tends to diverge from the straight line paths between the desired waypoints, further illustrated pictorially in Figure 10. The heading and displacement errors are shown in Figure 12, where positive error corresponds to a divergence along the left side of the reference track while the negative portion corresponds to a divergence along the right side of the reference track. The results show a maximum translational error of ±52 cm and a maximum rotational error of ±3 degrees approximately. The terrain negotiated by the robot during walking is shown in Figure 13 as a surface mesh generated using the contact point information. The color bar in Figure 13 represents the height of the terrain along the y axis.

A total of 25 simulation tests were conducted using the proposed FRC method. The simulation results are plotted in Figure 15 which represents the path traced by the robot. As apparent from Figure 15, both the CoM and ZMP profiles lie

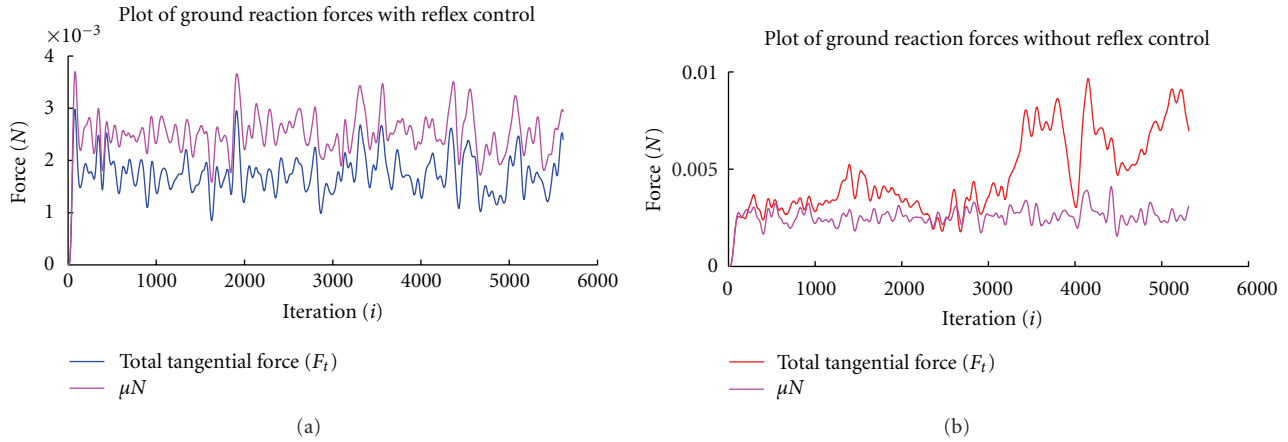

Figure 17: A Representation of ground forces in the two simulation tests.

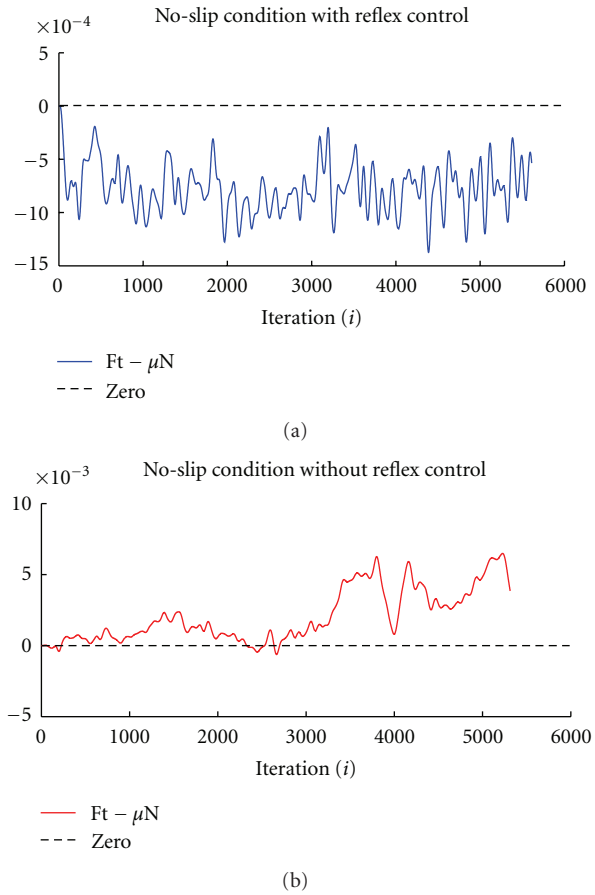

Figure 18: Plots of No-Slip condition in the two simulation tests.

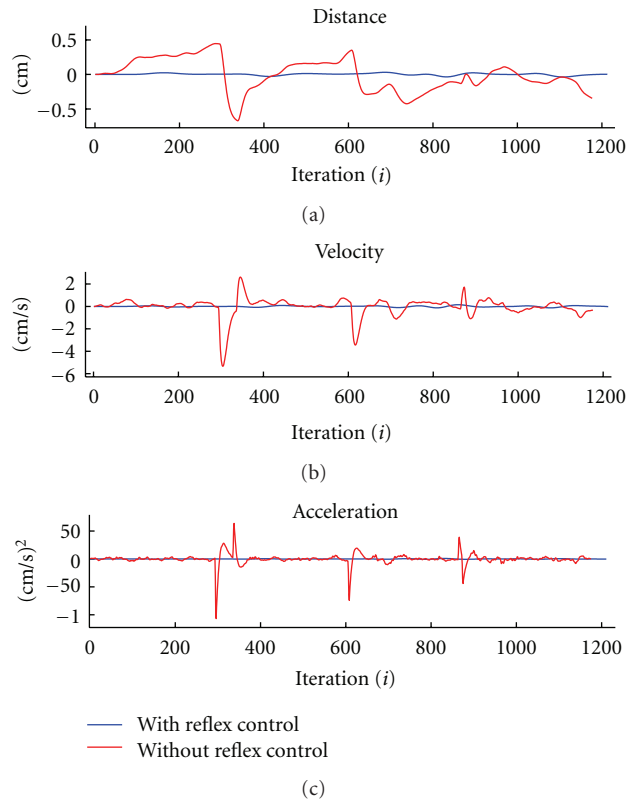

Figure 19: A comparative representation of disturbance estimation with and without using the proposed FRC method.

inside the Support Polygons on Surface satisfying the dynamic stability constraints and the path traced by the robot closely matches with the reference track as shown pictorially in Figure 14. The terrain explored by the robot is shown in Figure 16.

Figures 17, 18, and 19 demonstrate a comparative evaluation of the locomotion of the robot with and without using the proposed foothold reflex control method represented by blue and red plots respectively. Figure 17 shows a comparative representation of the estimated ground reaction forces. A close inspection of Figure 17(a) reveals that the total tangential force remains lesser than the normal reaction force times the combined coefficient of ground friction which validates the satisfaction of stability criterion throughout the robot's locomotion, further verified by the blue plot in Figure 18(a). Further evaluation of the simulation results reveals that the disturbances have significantly reduced when using the FRC method as shown in Figure 19. The attitude

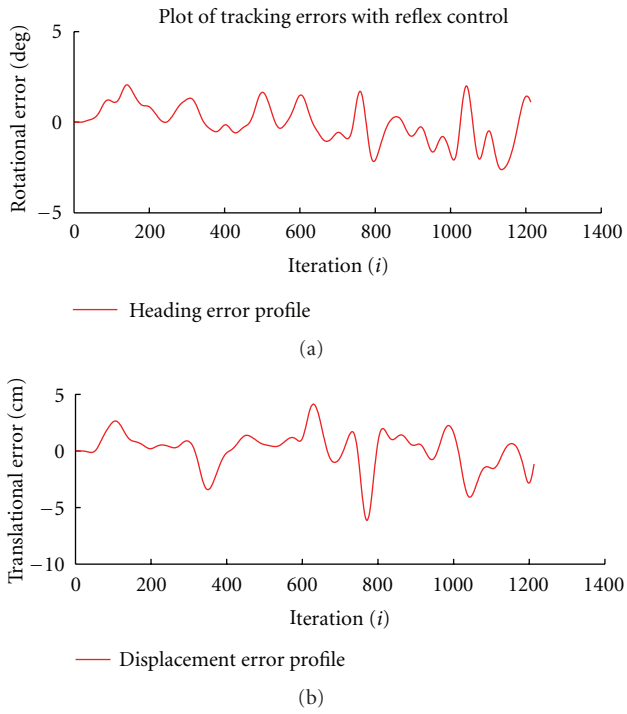

FIGURE 20: Tracking Errors using the proposed FRC method.

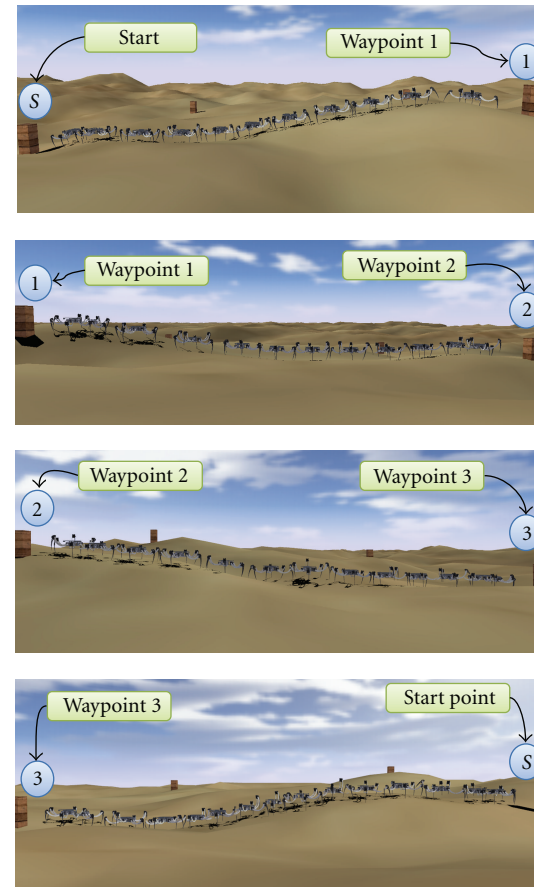

FIGURE 21: Locomotion of robot in visual simulation environment to show the body attitude control.

controller efficiently tracked the robot posture while walking as shown in Figure 21. Average speed of the robot was reduced from 0.33 m/sec to 0.32 m/sec using the proposed reflex control method however, the robot completed the course in relatively lesser time (3.5 mins as compared to 4 mins when not using the FRC method) with minimal tracking errors. The results reported in Figures 19 and 20 are considered satisfactory given the quality of the kinematic model and the precision of software sensors provided by the open dynamics engine.

5. Conclusion

The robot presented here is a hexapod to walk using a biologically inspired leg control system over an uneven terrain using a sensor-based traction control. Sensory network in a leg is responsible for influencing the direction and motion of each joint such that an evolving, adaptive, and reactive stepping pattern is realized through leg-environment interaction. Simulation tests that evaluated this gait model showed that the robot could clear raised and lowered obstructions over uneven surface which were within and beyond the nominal gait control variables (leg-lift and leg-stroke), as shown by the obstacle crossing testing results. The simulation testing of the proposed foothold reflex control method showed significant improvement in the robot's ability to track a reference path over an uneven terrain. The gait stability was ensured using the center of mass and zero moment point stability criterion. The novelty of the proposed navigation method thus lies in the successful implementation of a reflex-based gait generation with an ability to perform obstacle crossing and path following in irregular terrains with adequate stability and minimal tracking errors. Future work in this area will involve improving fusion of sensor data through advanced filtering and disturbance rejection techniques.

References

[1] Ö. Ekeberg, M. Blümel, and A. Büschges, "Dynamic simulation of insect walking," *Arthropod Structure and Development*, vol. 33, no. 3, pp. 287–300, 2004.

[2] R. J. Wood, "The first takeoff of a biologically inspired at-scale robotic insect," *IEEE Transactions on Robotics*, vol. 24, no. 2, pp. 341–347, 2008.

[3] D. Kühn, M. Römmermann, N. Sauthoff, F. Grimminger, and F. Kirchner, "Concept evaluation of a new biologically inspired robot "LittleApe"," in *IEEE/RSJ International Conference on Intelligent Robots and Systems (IROS '09)*, pp. 589–594, October 2009.

[4] S. Yu, S. Ma, B. Li, and Y. Wang, "An amphibious snake-like robot: design and motion experiments on ground and in water," in *IEEE International Conference on Information and Automation (ICIA '09)*, pp. 500–505, June 2009.

[5] M. Konyev, F. Palis, Y. Zavgorodniy et al., "Walking Robot Anton: Design, Simulation, Experiments," in *International Conference on Climbing and Walking Robots and the Support Technologies for Mobile Machines (CLAWAR '08)*, pp. 922–929, September 2008.

[6] A. Roennau, T. Kerscher, and R. Dillmann, "Design and kinematics of a biologically-inspired leg for a six-legged walking machine," in *3rd IEEE RAS and EMBS International Conference on Biomedical Robotics and Biomechatronics (BioRob '10)*, pp. 626–631, September 2010.

[7] Ch. Grand, F. Ben Amar, and F. Plumet, "Motion kinematics analysis of wheeled-legged rover over 3D surface with posture adaptation," in *Proceedings of the 12th IFToMM World Congress in Mechanism and Machine Science*, 2007.

[8] R. B. McGhee and G. I. Iswandhi, "Adaptive locomotion of a multi-legged robot over rough terrain," *IEEE Transactions on Systems, Man, and Cybernetics*, vol. 9, no. 4, pp. 176–182, 1979.

[9] R. B. McGhee, "Vehicular legged locomotion," in *Advances in Automation and Robotics*, N. Saridis, Ed., JAI, Greenwich, Conn, USA, 1985.

[10] K. J. Waldron and R. B. McGhee, "The adaptive suspension vehicle," *IEEE Control Systems Magazine*, vol. 6, no. 6, pp. 7–12, 1986.

[11] H. J. Chiel, R. D. Beer, R. D. Quinn, and K. S. Espenschied, "Robustness of a distributed neural network controller for locomotion in a hexapod robot," *IEEE Transactions on Robotics and Automation*, vol. 8, no. 3, pp. 293–303, 1992.

[12] P. V. Nagy, S. Desa, and W. L. Whittaker, "Energy-based stability measures for reliable locomotion of statically stable walkers. Theory and application," *International Journal of Robotics Research*, vol. 13, no. 3, pp. 272–287, 1994.

[13] J. M. Yang and J. H. Kim, "Fault-tolerant locomotion of the hexapod robot," *IEEE Transactions on Systems, Man, and Cybernetics, Part B*, vol. 28, no. 1, pp. 109–116, 1998.

[14] K. Inoue, T. Tsurutani, T. Takubo, and T. Arai, "Omni-directional gait of limb mechanism robot hanging from grid-like structure," in *IEEE/RSJ International Conference on Intelligent Robots and Systems (IROS '06)*, pp. 1732–1737, October 2006.

[15] W. A. Lewinger and R. D. Quinn, "BILL-LEGS: low computation emergent gait system for small mobile robots," in *IEEE International Conference on Robotics and Automation (ICRA '08)*, pp. 251–256, May 2008.

[16] R. Brooks, "A Robot that Walks: Emergent Behaviors from a Carefully Evolved Network," MIT AI Lab Memo 1091, February 1989.

[17] R. D. Beer, R. D. Quinn, H. J. Chiel, and R. E. Ritzmann, "Biologically inspired approaches to robotics," *Communications of the ACM*, vol. 40, no. 3, pp. 17–38, 1997.

[18] K. S. Espenschied, R. D. Quinn, R. D. Beer, and H. J. Chiel, "Biologically based distributed control and local reflexes improve rough terrain locomotion in a hexapod robot," *Robotics and Autonomous Systems*, vol. 18, no. 1-2, pp. 59–64, 1996.

[19] M. Frik, M. Guddat, M. Karatas, and C. D. Losch, "A novel approach to autonomous control of walking machines," in *Proceedings of the 2nd International Conference on Climbing and Walking Robots (CLAWAR '99)*, G. S. Virk, M. Randall, and D. Howard, Eds., pp. 333–342, Professional Engineering Publishing Limited, 1999.

[20] H. Cruse, J. Dean, U. Müller, and J. Schmitz, "The stick insect as a walking robot," in *Proceedings of the 5th International Conference on Advanced Robotics (ICAR '91)*, pp. 936–940, 1991.

[21] H. Cruse, T. Kindermann, M. Schumm, J. Dean, and J. Schmitz, "Walknet—a biologically inspired network to control six-legged walking," *Neural Networks*, vol. 11, no. 7-8, pp. 1435–1447, 1998.

[22] D. Hess and A. Büschges, "Sensorimotor pathways involved in interjoint reflex action of an insect leg," *Journal of Neurobiology*, vol. 33, no. 7, pp. 891–913, 1997.

[23] W. A. Lewinger, B. L. Rutter, M. Blümel, A. Büschges, and R. D. Quinn, "Sensory Coupled Action Switching Modules (SCASM) generate robust, adaptive stepping in legged robots," in *Proceedings of the 9th International Conference on Climbing and Walking Robots (CLAWAR '06)*, pp. 661–671, Brussels, Belgium, September 2006.

[24] W. A. Lewinger and R. D. Quinn, "A hexapod walks over irregular terrain using a controller adapted from an insect's nervous system," in *IEEE/RSJ International Conference on Intelligent Robots and Systems*, Taipei, Taiwan, October 2010.

[25] V. Dürr, J. Schmitz, and H. Cruse, "Behaviour-based modelling of hexapod locomotion: linking biology and technical application," *Arthropod Structure and Development*, vol. 33, no. 3, pp. 237–250, 2004.

[26] C. Yi, W. Shuxin, and L. Zhiqun, "The Robot's Working Space and Its Analytic Express Based on Random Possibility Mechanism Design and Study," vol. 2, pp. 1–4, 2005.

[27] Y. Yuwei and Z. Xinhua, "The Working Space and Agility Analysis of 3-RRRT Parallel Robot Mechanism Design," vol. 22, no. 2, pp. 11–13, 2005.

[28] K. Walas, D. Belter, and A. Kasinski, "Control and environment sensing system for a six-legged robot," *Journal of Automation, Mobile Robotics & Intelligent Systems*, vol. 2, no. 3, pp. 26–31, 2008.

[29] T. T. Lee, C. M. Liao, and T. K. Chen, "On the stability properties of hexapod tripod gait," *IEEE journal of robotics and automation*, vol. 4, no. 4, pp. 427–434, 1988.

[30] U. Asif and J. Iqbal, "Modeling and simulation of biologically inspired hexapod robot using SimMechanics," in *Proceedings of the IASTED International Conference, Robotics (Robo 2010)*, pp. 128–135, Phuket, Thailand, November 2010.

[31] X. Ke, Z. Gong, and J. Wu, "Study on walking stabilities of a biped robot in considering the distribution of ground reacting forces," in *IEEE International Conference on Mechatronics and Automation (ICMA '06)*, pp. 1636–1641, June 2006.

[32] C. Zhu and A. Kawamura, "What is the real frictional constraint in biped walking?—discussion on frictional slip with rotation," in *IEEE/RSJ International Conference on Intelligent Robots and Systems (IROS '06)*, pp. 5762–5768, October 2006.

[33] D. Belter, "Adaptive foothold selection for a hexapod robot walking on rough terrain," in *the 7th Workshop on Advanced Control and Diagnosis*, Zielona Gora, Poland, 2009.

[34] P. Labeçki, A. Lopatowski, and P. Skrzypczynski, "Terrain perception for a walking robot with a low-cost structured light sensor," in *Proceedings of the 4th European Conference on Mobile Robots*, pp. 199–204, Dubrovnik, Croatia, 2009.

[35] B. Gaßmann, L. Frommberger, R. Dillmann, and K. Berns, "Real-time 3D map building for local navigation of a walking robot in unstructured terrain," in *IEEE/RSJ International Conference on Intelligent Robots and Systems*, pp. 2185–2190, October 2003.

[36] C. Plagemann, S. Mischke, S. Prentice, K. Kersting, N. Roy, and W. Burgard, "Learning predictive terrain models for legged robot locomotion," in *IEEE/RSJ International Conference on Intelligent Robots and Systems (IROS '08)*, pp. 3545–3552, September 2008.

[37] A. Roennau, T. Kerscher, M. Ziegenmeyer, J. M. Zoellner, and R. Dillmann, "Six-legged walking in rough terrain based on foot point planning," in *Mobile Robotics: Solutions and Challenges*, pp. 591–598, World Scientific, Singapore, 2009.

[38] L. Mu and R. E. Ritzmann, "Interaction between descending input and thoracic reflexes for joint coordination in cockroach. II Comparative studies on tethered turning and searching," *Journal of Comparative Physiology A*, vol. 194, no. 3, pp. 299–312, 2008.

[39] J. R. Rebula, P. D. Neuhaus, B. V. Bonnlander, M. J. Johnson, and J. E. Pratt, "A controller for the LittleDog quadruped walking on rough terrain," in *IEEE International Conference on Robotics and Automation (ICRA '07)*, pp. 1467–1473, April 2007.

[40] P. Arena, L. Fortuna, M. Frasca, and L. Patané, "Sensory feedback in locomotion control," in *Dynamical Systems, Wave-Based Computation and Neuro-Inspired Robots*, vol. 500, pp. 143–158, Springer, Berlin, Germany, 2008.

[41] S. A.A. Moosavian and A. Dabiri, "Dynamics and planning for stable motion of a hexapod robot," in *IEEE/ASME International Conference on Advanced Intelligent Mechatronics (AIM '10)*, pp. 818–823, Montreal, Canada, July 2010.

[42] X. Ke, Z. Gong, and J. Wu, "Study on walking stabilities of a biped robot in considering the distribution of ground reacting forces," in *IEEE International Conference on Mechatronics and Automation (ICMA '06)*, pp. 1636–1641, Luoyang, China, June 2006.